

Percolation Transition of Persistent Photoconductivity in II-VI Mixed Crystals

H. X. Jiang and J. Y. Lin

Department of Physics, Cardwell Hall, Kansas State University, Manhattan, Kansas 66506-2601

(Received 27 November 1989)

We have observed for the first time conductivity fluctuations in the persistent photoconductivity mode in II-VI mixed crystals with the magnitude following the percolation approach as $|T - T_c|^{-\beta}$, where T_c is the percolation threshold temperature. Experimental results have demonstrated that the random local-potential fluctuations induced by compositional fluctuations are responsible for the persistent photoconductivity observed in II-VI mixed crystals. Different behaviors resulting from the DX centers, the macroscopic barrier, and the random local-potential fluctuations are distinguished.

PACS numbers: 72.20.Jv, 72.60.+g, 72.80.Ey

There has been a considerable amount of experimental and theoretical effort directed towards the understanding of persistent photoconductivity (PPC), which has been observed in a variety of semiconductors.¹ Several models have been proposed to explain the origin of PPC. In the microscopic local-potential fluctuation model, the separation of photoexcited carriers by random local-potential fluctuations (RLPF) was believed to be the origin of PPC.¹ Queisser and Theodorou have demonstrated for selectively doped GaAs-layered structures that the macroscopic barrier (MB) due to band bending at the interface between layer and substrate leads to PPC.^{2,3} The other dominant mechanism involves photoexcitation of electrons from deep traps (DX centers) which undergo a large lattice relaxation.^{4,5} In this Letter, we report direct experimental observations on the percolation transition in PPC which strongly support our recent model that RLPF induced by compositional fluctuations are the origin of the PPC observed in II-VI mixed semiconductor crystals.⁶

The II-VI mixed crystals used here are *undoped* $Zn_{0.3}Cd_{0.7}Se$ and $CdS_{0.5}Se_{0.5}$ with dark room-temperature resistivity of about $10^9 \Omega \text{ cm}$. The growth method was described previously.⁶ The defect-center (DX centers) induced PPC effect is also investigated for a $2\text{-}\mu\text{m}$ epitaxy layer of $Al_{0.3}Ga_{0.7}As$ which is doped with $3.3 \times 10^{17} \text{ cm}^{-3}$ Si, grown on a semi-insulating GaAs(100) substrate. The decay curves obtained at different conditions were taken in such a way that the system was heated up to about 300 K to convert the illuminated sample to its initial state and then cooled down again in darkness to the temperature of the measurements. Ohmic contacts of 1-mm diameter and about 7 mm apart were formed using indium solder for II-VI mixed crystals and by indium alloying (400°C , 20 min) for $Al_{0.3}Ga_{0.7}As$. The junctions were carefully tested for Ohmic contacts.

For the $Zn_{0.3}Cd_{0.7}Se$ mixed crystal, virtually no PPC could be observed at $T < 70 \text{ K}$ and the PPC relaxation behavior is well described by the stretched-exponential function at temperature $T < 220 \text{ K}$. In Fig. 1, we show scaled PPC decay curves obtained at 170 K for

$Zn_{0.3}Cd_{0.7}Se$ after photoexcitation with four different excitation photon doses, which can be expressed as

$$I_{PPC}(t') = I_{PPC}(0) \exp(-t'^{\beta}), \quad (1)$$

where the scaled time is $t' = t/\tau$, with τ being the characteristic relaxation time constant obtained for the different photon doses. We see that the scaled PPC de-

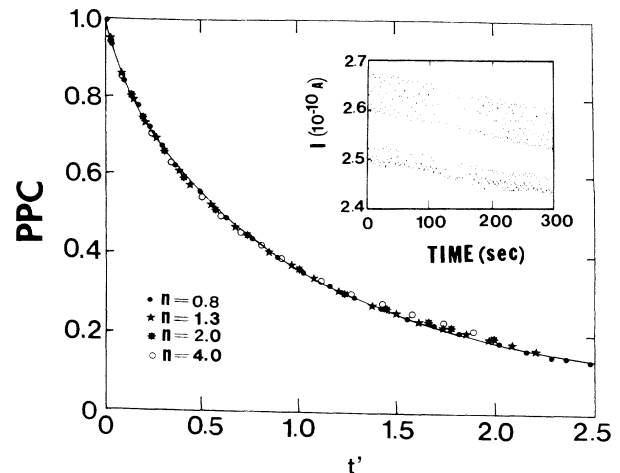


FIG. 1. Scaled PPC decay curves obtained at 170 K for $Zn_{0.3}Cd_{0.7}Se$ after illumination with four different excitation photon doses. Each curve is normalized to unity at $t=0$, the moment at which light illumination is terminated; the dark current has been subtracted out. The unit of the excitation photon dose n is $10^{16} \text{ photons/cm}^2$. The characteristic relaxation time constant τ increases with an increase of n and is 604, 679, 734, and 776 s for the four n values shown here. $t' (=t/\tau)$ is the scaled time, where the scale factors used are the corresponding values of τ obtained for the four different excitation photon doses. The solid line is a plot of a stretched-exponential function $I(t') = I(0) \exp(-t'^{\beta})$ with $\beta = 0.77$. Inset: Representative plots of PPC noise measured at two different temperatures after warmup from 8 K for $CdS_{0.5}Se_{0.5}$. The sample has been illuminated with light intensity of about $2 \times 10^{13} \text{ photons/cm}^2$ for 500 s at 8 K. The data with larger fluctuations in PPC correspond to the measurements obtained at 15 K, while the data with smaller fluctuations are obtained at 13 K. $t=0$ is arbitrary.

cay curves obtained for different excitation photon doses are fitted by a *single* stretched-exponential function with $\beta=0.77$ shown as the solid line. Thus the properties of PPC decay following the stretched-exponential function and of excitation-photon-dose independence of the decay parameter β are demonstrated. Furthermore, in the temperature region $125 \text{ K} < T < 220 \text{ K}$, the temperature-dependent PPC buildup level after excitation with the same amount of photon dose follows the percolation approach as $I_{\text{PPC}}(T, t=0) \propto (T - T_C)^{\mu'}$, with a transition temperature of $T_C \approx 118 \text{ K}$ and a conductivity exponent obtained via temperature of $\mu' \approx 1.3$. The temperature-dependent decay parameter $\tau(\beta)$ also depicts a sharp increase (decrease) near 120 K, which indicates the same transition occurring near 120 K.⁶ Similar PPC behavior is also observed for higher-quality (lower degree of the compositional fluctuations) $\text{CdS}_{0.5}\text{Se}_{0.5}$ mixed crystals, in which a transition temperature near 15 K is deduced under the same experimental conditions.⁷

The stretched-exponential function usually describes the relaxation of a wide class of disordered systems toward equilibrium.⁸ In mixed crystals, large compositional fluctuations are well known, which cause potential fluctuations in band edges and the exciton emission linewidth to broaden.^{9,10} Thus the decay behavior and the percolation phenomena exhibited by II-VI mixed crystals suggest RLPF induced by compositional fluctuations are responsible for PPC. In this model description, photoexcited electrons (holes) are localized at the low-potential sites in the conduction (valence) band. Spatially, the low-potential sites in the conduction band are separated from those in the valence band, leading to very long carrier lifetimes. Below T_C , the electrons hopping between local potential minima induce low-level PPC, and the electron transport becomes negligible at very low temperatures. As temperature increases to above T_C , the accessible electron sites form a percolation network and electrons experience a transition from localized to percolation (delocalized) states, in which case conductivity is contributed by electrons percolating through the network of accessible states. The scaling behavior in Fig. 1 suggests a fractal structure for the network of percolation-accessible sites of electrons. The decay exponent β is independent of excitation photon dose and thus depends only on the fractal dimension.

In undoped II-VI semiconductors, an intrinsic lattice defect may act as donor or acceptor, similar to the case of a foreign impurity atom. Therefore, one might ask whether these defects which may have a thermal capture barrier due to lattice relaxation could cause the PPC effect involved in our observation. To answer this, we performed comparison experiments on a $\text{Al}_{0.3}\text{Ga}_{0.7}\text{As}$ sample in which the defects (*DX* centers) are a well-known cause of a strong PPC effect at temperatures $T < 150 \text{ K}$. The PPC relaxation time constant τ as a function of temperature is systematically measured. Figure 2 shows the temperature dependences of τ for both

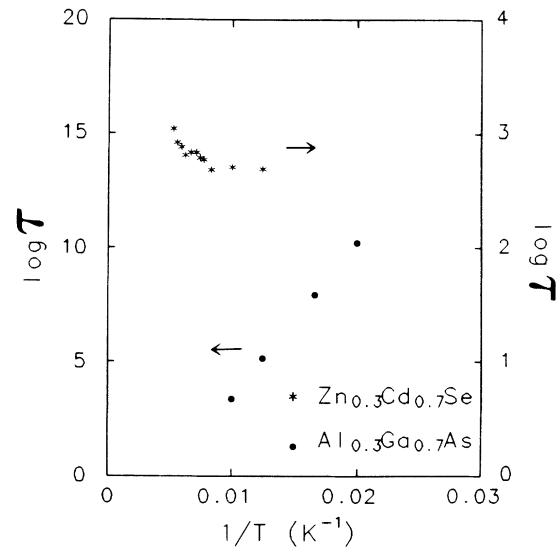


FIG. 2. Plot of $\log_{10}\tau$ vs $1/T$ for $\text{Al}_{0.3}\text{Ga}_{0.7}\text{As}$ (●'s) and $\text{Zn}_{0.3}\text{Cd}_{0.7}\text{Se}$ (*'s). Excitation intensity and exposure time used are, respectively, about 10^{14} photons/cm²s and 100 s for $\text{Al}_{0.3}\text{Ga}_{0.7}\text{As}$ and about 2×10^{13} photons/cm²s and 1000 s for $\text{Zn}_{0.3}\text{Cd}_{0.7}\text{Se}$.

$\text{Zn}_{0.3}\text{Cd}_{0.7}\text{Se}$ and $\text{Al}_{0.3}\text{Ga}_{0.7}\text{As}$ samples. We see that for $\text{Al}_{0.3}\text{Ga}_{0.7}\text{As}$, τ is *thermally activated* [i.e., $\tau = a \times \exp(E_b/kT)$] in the measured temperature region of $T > 40 \text{ K}$ since the decay of PPC in this sample is due to electron capture at the defect centers. E_b obtained from Fig. 2 is about 160 meV and τ decreases with increase of T in the entire region, consistent with previous experiments.^{4,5,12} For $\text{Zn}_{0.3}\text{Cd}_{0.7}\text{Se}$, τ has no activated temperature dependence and, more strikingly, τ increases with increase of temperature in the corresponding region of interest, which has been interpreted in terms of the effect of electron redistribution in percolation sites,⁶ and hence rules out the possibility that the defects could induce the PPC effect in this sample. These results support our interpretation that RLPF induced by compositional fluctuations are responsible for PPC observed in II-VI mixed crystals. Other supporting evidence for the RLPF model is the observation of a sharp PPC transition occurring near 1.5 K in a compensated crystalline bulk CdS single crystal.¹³ T_C occurring at much lower temperatures in compensated crystalline semiconductors can be understood in that the degree of the fluctuations due to inhomogeneous impurity distributions is much lower than for those due to compositional fluctuations.

In addition to the above observations, we also observe the strongest experimental evidence which supports our model described above. We find that the magnitude of the conductivity noise in the PPC in II-VI mixed crystals follows the percolation approach as $|T - T_C|^{-\kappa}$ and reaches a maximum value at the critical temperature T_C . To our knowledge, this is the first conclusive experimental observation of conductivity noise in the PPC mode

which directly demonstrates that RLPF are responsible for the PPC observed in II-VI mixed crystals. The noise data are obtained in the following steps: First, we cool the sample down from room temperature to 8 K in the darkness and illuminate the sample at 8 K for 500 s at an intensity of about 2×10^{13} photons/cm²s to generate charge carriers; then we allow the illuminated sample to warm up, without converting it to its initial state, to the temperature of the measurements. The time resolution in the inset of Fig. 1 is 1 point/s. The noise signal is more difficult to observe in the usual decay curves such as those in Fig. 1 because the current levels are much higher immediately after illumination. In the inset of Fig. 1, we show experimental data on PPC noise obtained at two representative temperatures for a CdS_{0.5}Se_{0.5} mixed crystal. We see that the magnitude of the PPC noise obtained with 1-s time resolution using the above-described method is nearly time independent and depends only on temperature. In contrast, no noise in the PPC mode is observed for Al_{0.3}Ga_{0.7}As materials. The conductivity noise in semiconductors is believed to be caused by fluctuations of the number and mobility of electrons in the percolation network.¹⁴ Rammal and co-workers theoretically predicted for an ideal system that the magnitude of the relative noise diverges as $(p - p_C)^{-\kappa}$ when one approaches the percolation threshold p_C , where κ is a new exponent.^{15,16}

Here, we concentrate on the behavior of the magnitude of the PPC noise in CdS_{0.5}Se_{0.5} and Zn_{0.3}Cd_{0.7}Se mixed crystals. The average fluctuation width of the PPC data obtained at different temperatures, such as those in the inset of Fig. 1, represents the magnitude of the PPC noise in the low-frequency region. The magnitude of the PPC noise as a function of temperature is

shown in Fig. 3 and Fig. 4, respectively, for Zn_{0.3}Cd_{0.7}Se and CdS_{0.5}Se_{0.5} mixed crystals. The most significant feature is that the magnitude of the PPC noise indeed reaches a maximum value near 120 K for Zn_{0.3}Cd_{0.7}Se and 15 K for CdS_{0.5}Se_{0.5}. The discrepancy between the experimental results and the theoretical prediction^{15,16} at the critical temperatures can be accounted for by the theoretical prediction being based on an ideal system. Physically, this behavior is due to the fact that as we approach the transition temperature, an infinite cluster is formed with only a few paths available for current conduction. Additionally, the magnitude of the PPC noise follows a power-law dependence on temperature,

$$\Delta I = \begin{cases} \alpha_1 (T - T_C)^{-\kappa'_1} & (T > T_C), \\ \alpha_2 (T_C - T)^{-\kappa'_2} & (T < T_C), \end{cases} \quad (2)$$

which is an outstanding feature of the percolative system. Here κ' is the noise exponent obtained via temperature. The solid lines in Figs. 3 and 4 are the plots of Eq. (2) with $T_C = 118$ K, $\alpha_1 = 1.64$, $\alpha_2 = 4.89$, $\kappa'_1 = 0.37$, and $\kappa'_2 = 0.47$ for Zn_{0.3}Cd_{0.7}Se (Fig. 3) and $T_C = 15$ K, $\alpha_1 = 7.48$, $\alpha_2 = 7.19$, $\kappa'_1 = 0.56$, and $\kappa'_2 = 0.57$ for CdS_{0.5}Se_{0.5} (Fig. 4), respectively, with the unit of ΔI being pA. To date, this is the first experimental attempt to measure the conductivity noise in the PPC mode. The observation of PPC noise provides the possibility of studying the conductivity noise in percolative semiconductors near the percolation threshold, with the additional advantage of the long relaxation time of the conductivity. T_C occurring at a lower temperature for the higher-quality CdS_{0.5}Se_{0.5} sample is consistent with the RLPF model.

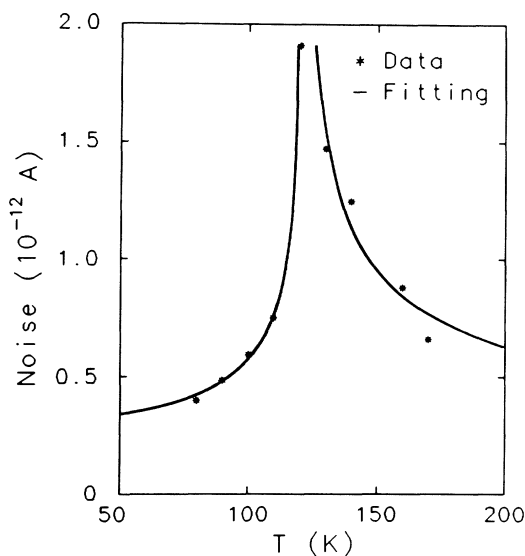


FIG. 3. The magnitude of the PPC noise vs temperature for a Zn_{0.3}Cd_{0.7}Se mixed crystal. The solid curves are the plot of Eq. (2) with $T_C = 118$ K.

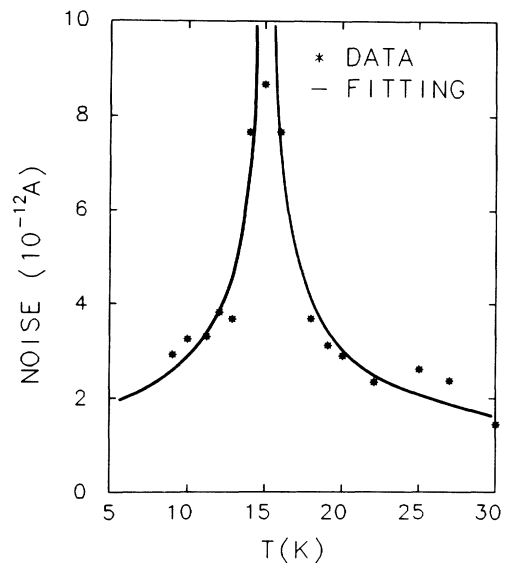


FIG. 4. The magnitude of the PPC noise vs temperature for a CdS_{0.5}Se_{0.5} mixed crystal. The solid curves are the plot of Eq. (2) with $T_C = 15$ K.

TABLE I. Properties of the three major PPC models which include the large-lattice-relaxation (LLR) model (Ref. 4), the macroscopic-barrier (MB) model (Ref. 2), and the random local-potential fluctuations (RLPF) model. T_U and T_L , respectively, indicate the upper and the lower temperature limits for existence of PPC. σ denotes PPC.

	LLR	MB	RLPF
Origin	Deep level traps	Interface potential	Microscopic inhomogeneity
Decay kinetics	Not well established ^a	$\Delta\sigma(t) = \Delta\sigma_0 - A \ln(t/\tau)$	$\sigma(t) = \sigma_0 \exp[-(t/\tau)^\beta]$
Key parameter	Height of the thermal barrier (E_b)	Carrier sheet density (nd)	Transition temperature (T_C)
PPC temperature region	$T < T_U^{LLR}$	$T < T_U^{MB}$	$T_L^{RLPF} < T < T_U^{RLPF}$
Transport mechanism	Conduction-band electrons	2D charge carriers	$T < T_C$ (hopping) $T > T_C$ (percolation)
Predicted phase transitions	None	None	Localization-to-percolation transition

^aReference 17.

We should indicate that the conductivity and noise exponents here are obtained via temperature, $T - T_C$, but not directly measured via the fraction of the electron accessible sites belonging to the infinite cluster, $p - p_C$. Therefore, the exponents μ' and κ' obtained here cannot be directly compared to the existing values in the literature on percolation. The correlation between T and p is unknown at this stage. However, we expect that T and p should not just simply follow a linear relationship, which is supported by the fact that both values of μ' and κ' are lower than the published values of μ and κ . Additionally, the magnitude of the PPC noise here is effectively measured from peak to peak in the low-frequency region, which may also lead to different values for noise exponents. The difference in the noise exponents κ' obtained for two different samples may be due to the fact that the relation between T and P is not universal, but sample dependent. A possible cause could be that different samples have different distributions of the tail states which is one of the factors for determining the correlation between T and p near the threshold. Furthermore, limited by the time response of about 1 s of our electrometer, which is suitable for measuring PPC in high-resistivity II-VI semiconductors, the frequency dependence of noise in the PPC mode cannot be studied yet, but will be investigated in the near future.

The observed PPC effect cannot be interpreted in terms of either the LLR model or the MB model which predicts no phase transition of any kind and that τ decreases with an increase of temperature. We summarize the different behaviors of PPC in the LLR, MB, and RLPF models in Table I, to distinguish the different origins for PPC. We see that very different PPC behaviors resulting from the three origins are evident, and that PPC behavior exhibited by II-VI mixed crystals is only consistent with the RLPF model.

In conclusion, we have observed conductivity noise in PPC in II-VI mixed crystals and its magnitude follows

the percolation approach and reaches a maximum value at T_C , which demonstrates that the random local-potential fluctuations induced by compositional fluctuations are responsible for the PPC observed in II-VI mixed crystals.

¹M. K. Sheinkman and A. Ya. Shik, *Fiz. Tekh. Poluprovodn.* **10**, 209 (1976) [*Sov. Phys. Semicond.* **10**, 128 (1976)].

²H. J. Queisser and D. E. Theodorou, *Phys. Rev. B* **33**, 4027 (1986).

³H. J. Queisser, *Phys. Rev. Lett.* **54**, 234 (1985).

⁴D. V. Lang and R. A. Logan, *Phys. Rev. Lett.* **39**, 635 (1977).

⁵D. V. Lang, R. A. Logan, and M. Joros, *Phys. Rev. B* **19**, 1015 (1979).

⁶H. X. Jiang and J. Y. Lin, *Phys. Rev. B* **40**, 10025 (1989).

⁷J. Y. Lin, S. X. Huang, G. Brown, and H. X. Jiang (to be published).

⁸R. G. Palmer, D. L. Stein, E. Abraham, and P. W. Anderson, *Phys. Rev. Lett.* **53**, 958 (1984).

⁹S. Permogorov, A. Reznitsky, S. Verbin, and V. Lysenko, *Solid State Commun.* **47**, 5 (1983).

¹⁰J. A. Kash, A. Ron, and E. Cohen, *Phys. Rev. B* **28**, 6147 (1983).

¹¹J. Y. Lin and H. X. Jiang, *Phys. Rev. B* **41**, 5178 (1990).

¹²R. J. Nelson, *Appl. Phys. Lett.* **31**, 351 (1977).

¹³D. Baum, J. Y. Lin, and A. Honig, *Bull. Am. Phys.* **33**, 301 (1988).

¹⁴M. B. Weissman, *Rev. Mod. Phys.* **60**, 537 (1988).

¹⁵R. Rammal, C. Tannous, and A. M. S. Tremblay, *Phys. Rev. A* **31**, 2662 (1985).

¹⁶R. Rammal, C. Tannous, P. Breton, and A. M. S. Tremblay, *Phys. Rev. Lett.* **54**, 1718 (1985).

¹⁷See, for example, P. M. Mooney, N. S. Caswell, and S. L. Wright, *J. Appl. Phys.* **62**, 4786 (1987); J. C. Bourgoin, S. L. Feng, and H. J. von Bardeleben, *Appl. Phys. Lett.* **53**, 1841 (1988); A. C. Campbell and B. G. Streetman, *Appl. Phys. Lett.* **54**, 445 (1989).